Nanorod-Direct Oriented Attachment Growth and Promoted Crystallization Processes Evidenced in Case of $ZnWO_4$

Biao Liu,[†] Shu-Hong Yu,*[,†] Linjie Li,[†] Fen Zhang,[†] Qiao Zhang,[†] Masahiro Yoshimura,[‡] and Peikang Shen[§]

Hefei National Laboratory for Physical Sciences at Microscale, Department of Materials Science and Engineering, University of Science and Technology of China, Hefei 230026, P. R. China, Center for Materials Design, Materials and Structures Laboratory, Tokyo Institute of Technology, 4259 Nagatsuta, Midori-ku, Yokohama 226-8503, Japan, and School of Physics and Engineering, Zhongshan University, Guangzhou 510275, P. R. China

Received: October 15, 2003; In Final Form: December 20, 2003

Single-crystal $ZnWO_4$ nanorods can direct the self-aggregation of the amorphous nanoparticulates and promote the crystallization and transformation process of the amorphous nanoparticulates derived from a simple supersaturation precipitation reaction in a nanorod/amorphous nanoparticle coexisting system under refluxing conditions or mild hydrothermal conditions. In this system, the obvious nanorod-direct epitaxial aggregation process in the case of $ZnWO_4$ was clearly observed instead of the traditional Ostwald ripening process. This finding could be universal to various oxide systems or even non-oxide systems. Such spontaneous self-aggregation and crystallization induced by the well-crystallized nanorods could provide a unique route for improving the property of an anisotropic material due to their rough surface structures made of tiny nanoparticle building blocks and could be used for the formation of more complex crystalline three-dimensional structures in which the branching sites could be added as individual nanoparticles.

Solution synthesis has been acting as an important synthetic route for the synthesizing nanoparticles with specific shape, sizes, orientation, etc., which play a key role in tailoring the properties of nanomaterials. Traditional solution synthetic methods have been widely used for the controlled synthesis of various colloidal nanoparticles.[1] One basic crystal growth mechanism in solution systems is the well-known "Ostwald ripening process".[2] In the Ostwald ripening process, the formation of tiny crystalline nuclei in a supersaturated medium occurs first and then is followed by crystal growth, in which the larger particles will grow at the cost of the small ones due to the energy difference between large particles and the smaller particles of a higher solubility based on the Gibbs−Thompson law. [3] Another growth mechanism involving mostly oriented particle aggregation,[4−7] which was termed conceptually as "oriented attachment" by Penn and Banfield et al.,[8−12] has emerged recently as highlighted by Alivisatos.[13] An increasing number of examples, which are relevant to such a mechanism, have been reported such as α-Fe_2O_3,[4,5] Au,[6] hydroxyapatite ($Ca_{10}(PO_4)_6(OH)_2$),[14] TiO_2,[7−9] FeOOH[11] and CoOOH,[12] and ZnS.[15] In this mechanism, the bigger particles are grown from small primary nanoparticles through an orientated attachment process, in which the adjacent nanoparticles are self-assembled by sharing a common crystallographic orientation and docking of these particles at a planar interface.[9] In addition, Averback et al. independently identified a similar spontaneous self-assembly process which they called "contact epitaxy" in dry state in contrast to the solution system during their studying of the deposition of Ag nanoparticles onto Cu substrate.[16,17]

Increasing evidence in several systems has been gradually observed for either directed particle aggregation or undirected particle aggregation. This kind of growth mode could lead to the formation of faceted particles or anisotropic growth if it occurs near equilibrium and there is sufficient difference in the surface energies of different crystallographic faces.[11] It is possible to form highly anisotropic crystals with perfection which clearly show the growth via oriented attachment as impressively evidenced for TiO_2.[8,9] Penn and Banfield confirmed that both anatase[8] and iron oxide nanoparticles[10] with sizes of a few nanometers can coalesce under hydrothermal conditions by the oriented attachment process. A recent observation shows that the oriented attachment can also control the coarsening of mercaptoethanol-capped ZnS nanoparticles even though the organic ligands will control the aggregation state of the nanoparticles during the hydrothermal treatment.[15] A very recent report by Weller et al provided some strong evidence that perfect ZnO nanorods can be conveniently self-assembled from small ZnO quasi-spherical nanoparticles based on the oriented attachment mechanism by the evaporation and reflux of a solution containing 3−5 nm nanoparticles.[18] Previous observations of self-organization or directed-aggregation of nanoparticles into ordered structures mainly relies on a special binding interaction of the bridging ligands capped on the surface of nanoclusters. For example, the self-alignment of acetate and thiolates capping agent protected CdS nanoclusters with the empirical formula $Cd_4S_1RS_{2.9}(CH_3COO)_{1.32}$ into chain structures or 2D thin films was observed by Chemseddine et al.[19] However, recent advances show that even unstabilized nanoparticles can spontaneously self-organize into perfect nanostructures as demonstrated by

* To whom correspondence should be addressed. E-mail: shyu@ustc.edu.cn. Fax: 0086 551 3603040.
[†] University of Science and Technology of China.
[‡] Tokyo Institute of Technology.
[§] Zhongshan University.

10.1021/jp037129q CCC: $27.50
Published on Web 02/05/2004

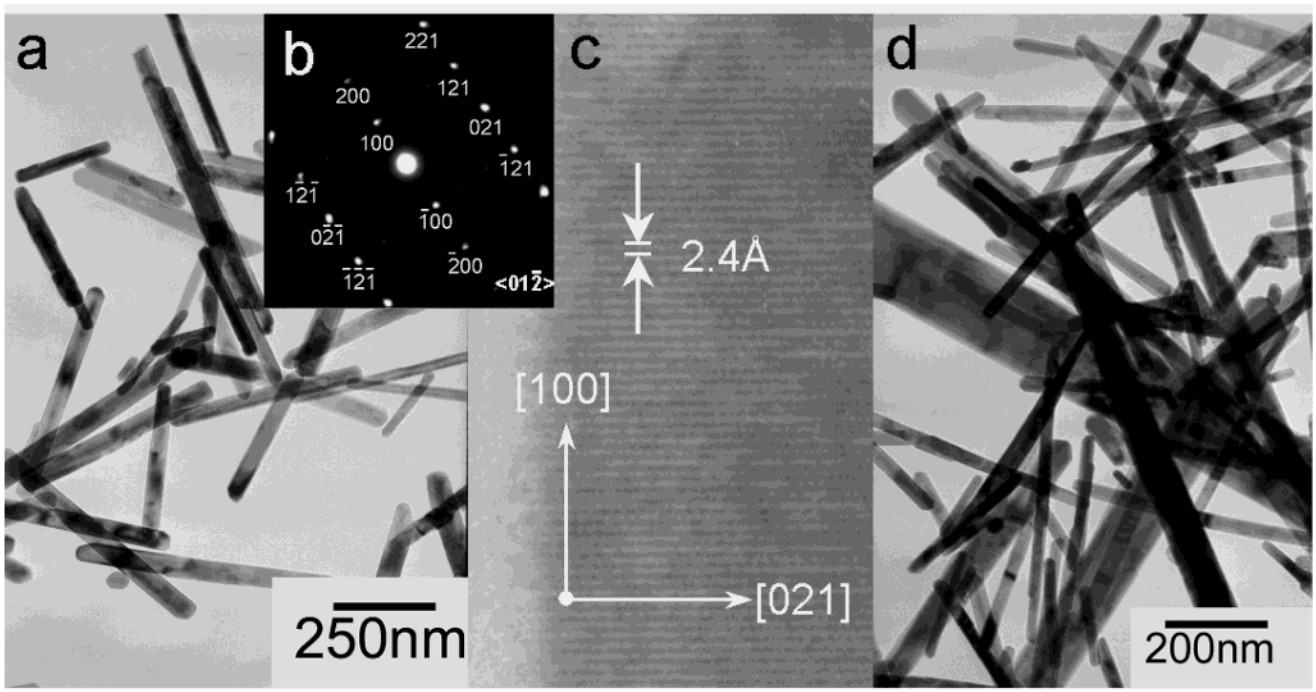

Figure 1. (a) Typical $ZnWO_4$ nanorods synthesized at 180 °C for 12 h, pH 8. (b) ED pattern of the nanorods. (c) HRTEM image of the nanorods. (d) TEM images of the $ZnWO_4$ nanorods after hydrothermal ripening at 180 °C for 36 h.

Kotov et al. in the case of the formation of CdTe nanowires self-organized from individual nanoparticles.[20]

In addition, above aggregation-based growth mechanisms could provide a unique route for the incorporation of defects, such as edge and screw dislocations, in stress-free and initially defect-free nanocrsytalline materials,[9] which could improve the reactivity of the nanocrystalline subunits. Although so far there are only few reports on the oriented attachment of nanoparticles, this new growth mechanism could offer an additional tool to design advanced materials with anisotropic material property and could be used for the synthesis of more complex crystalline three-dimensional structures in which the branching sites could be added as individual nanoparticles.[13,18]

Metal tungstates and molybdates are two important families of inorganic materials with strong application potential in various fields because of their intriguing luminescence behavior, structural properties and potential applications[21] such as heterogeneous catalysis.[22] Recently, we have demonstrated that a family of tungstate nanorods/nanowires can be conveniently synthesized in a surfactant (or ligand)-free solution system through a simple solution process at room temperatures and at elevated temperature by a hydrothermal process.[23]

In this letter, we report new evidence for the oriented attachment mechanism in which the nanorods obviously act as an epitaxial "substrate" or guide the directional aggregation process for the formation of nanorods based aggregated structures. In addition, the presence of the single-crystal nanorods was also found to be favorable for the promotion of crystallization and transformation of amorphous nanoparticulates. The influence of reaction conditions either under refluxing or hydrothermal conditions on the shape, size of the nanorods, phase, and structure evolution was discussed. To our best knowledge, the evidence of the nanorod-guided self-aggregation of tiny nanoparticles has not been reported previously.

Analytical grade $Na_2WO_4 \cdot 2H_2O$ and $ZnCl_2$ were purchased from Shanghai chemical industrial company and were used without further purification. The $ZnWO_4$ nanorods were synthesized in a 60 mL capacity Teflon-lined stainless steel autoclave, which was done in a digital type temperature controlled oven. The detailed synthetic procedures of pure $ZnWO_4$ nanorods have been described previously.[23] The nanorods guided aggregation experiments were performed in a flask with mild magnetic stirring and aging for different periods. Typically, 0.2 mmol $ZnWO_4$ nanorods synthesized at 180 °C for 24 h were added into a flask containing 40 mL of water and refluxing for different periods at 120 °C after adding 1 mL of 0.2 M $ZnCl_2$ and 1 mL of 0.2 M Na_2WO_4. The pH was adjusted using diluted HCl and NaOH to the desirable value. To follow the crystal growth process, the samples were taken at different time intervals. For comparison, the crystallization of a fresh mixture made of a $ZnCl_2$ and Na_2WO_4 solution in the presence of single-crystal $ZnWO_4$ nanorods under hydrothermal conditions at different temperature was also performed in a Teflon innered autoclave.

The products were characterized by X-ray diffraction patterns (XRD), recorded on a MAC Science Co. Ltd. MXP 18 AHF X-ray diffractometer with monochromatized Cu Kα radiation ($\lambda = 1.54056$ Å); transmission electron microscopy (TEM) and high-resolution transmission electron microscopy (HRTEM), performed on a Hitachi (Tokyo, Japan) H-800 transmission electron microscope (TEM) at an accelerating voltage of 200 kV, and a JEOL-2010 high-resolution transmission electron microscopy (HRTEM), also at 200 kV, respectively.

$ZnWO_4$ nanorods with an average diameter of 40 nm and length up to 500 nm were synthesized through a hydrothermal crystallization process as shown in Figure 1a. The nanorods were perfect single crystals with straight and extended rod shapes. The HRTEM image (Figure 1c) shows that the nanorods with perfect edges free of lattice are structurally uniform with an interplanar spacing of about 2.4 Å, corresponding to the (200) lattice spacing of $ZnWO_4$. The indexed select electron diffraction pattern for the $\langle 01\bar{2} \rangle$ zone reveals the single crystal nature of the nanorods and further confirmed that the nanorods grow preferentially along [100] direction which is parallel to (021) faces.

The conventional hydrothermal crystallization process or transformation process with amorphous nanoparticles as precur-

SCHEME 1. Formation Process of the Nanorods by Hydrothermal Crystallization Process

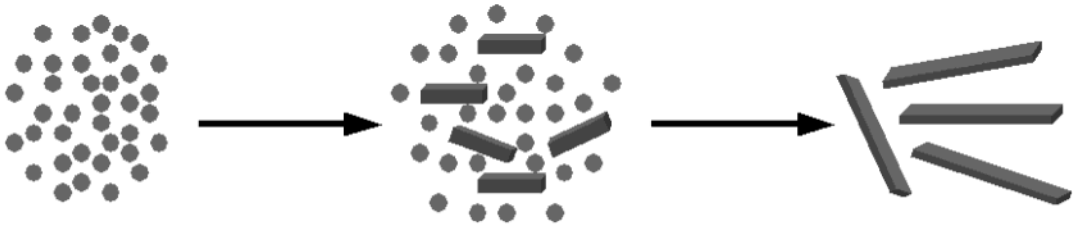

(i) Primary amorphous particulates

(ii) Formation of nanorods by hydrothermal activated intrinsically anistropic growth at the cost of small particulates

(iii) Ripened nanorods/nanowires

sors is a typical Oswald ripening process, in which a highly supersaturated solution is adopted and amorphous fine particulates act as the precursor. In this mechanism, the formation of tiny crystalline nuclei in a supersaturated medium occurred at first and then followed by crystal growth. The larger particles will grow at the expense of the small ones due to the difference between large particles and the smaller particles of a higher solubility according to the well-known Gibbs−Thomson law. In the early stage, the examination of intermediate products shows the coexistence of the short rods and irregular nanoparticles. With the reaction going on, the irregular nanoparticles vanished and the longer nanorods formed, suggesting that the longer nanorods obviously grew at the expense of smaller particulates. The formation process of nanorods/nanowires can be schematically illustrated in Scheme 1.

Refluxing of a fresh mixture of $ZnCl_2$ and Na_2WO_4 solutions in the presence of a suitable amount of single-crystal $ZnWO_4$ nanorods (0.2 mmol) at 120 °C for different reaction times produced pure $ZnWO_4$ nanorods with typical shapes as shown in Figure 2. Figure 2 indicated that all small nanoparticles tend to attach on the backbone of the nanorods. It is interesting that no individual nanoparticles in a dispersed way were found in the solution under the present conditions even though the samples were ultrasonically treated for preparation of TEM grids. Electron diffraction patterns of the nanorods as shown in Figure 2d taken along $\langle 01\bar{1} \rangle$ zone axis confirmed that the nanorods are the perfect single crystals.

The perfect parallel fringes without the misorientations observed by the high magnification TEM (HRTEM) (Figure 3) shows that all small nanoparticles are attached on the nanorods with the same orientation as the uniaxial nanorods. Lattice resolved HRTEM images in Figure 3b−d clearly show that all of the outlayers of the rods are composed of tiny nanoparticles with the same orientation along the [100] direction as that observed for the untreated $ZnWO_4$ nanorods. The lattice space was about 4.9 Å, corresponding to the interplanar spacing of (001) planes for $ZnWO_4$. Again, the HRTEM observation from the different parts of the nanorods confirmed that all nanoparticles have the same orientation as the extended nanorods, underlying that the nanorods presented in the solution can direct the self-aggregation of the tiny nanoparticles presented in the solution.

The fact that the crystal lattice planes are perfectly aligned shows that dislocations at the contact areas between the adjacent particles, which lead to defects in the finally formed bulk crystals, can be avoided. Furthermore, the nanorods with rather rough surfaces made of small primary building blocks were still perfect single crystals as confirmed by the electron diffraction patterns shown in Figure 2d, corresponding to the results of X-ray diffraction pattern (see Figure 4b).

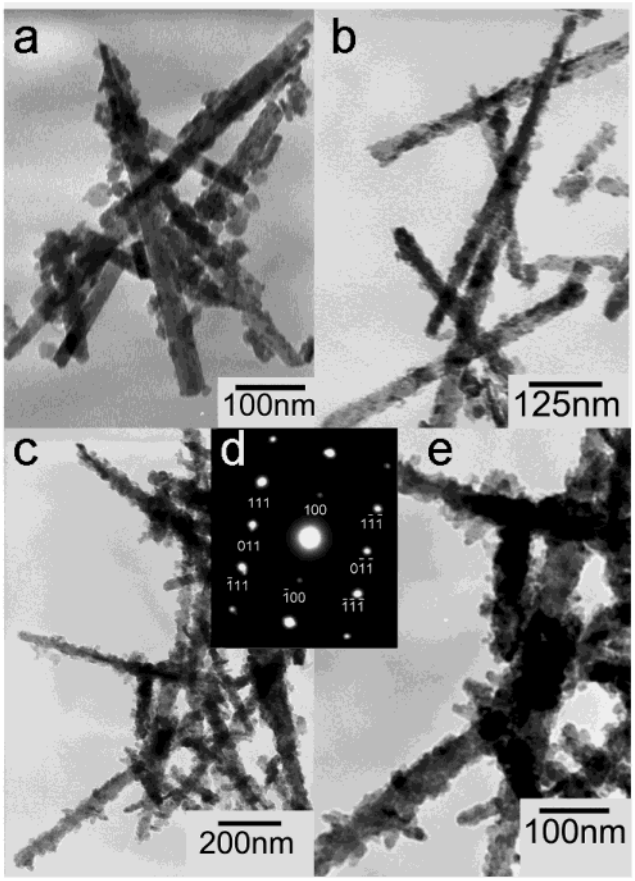

Figure 2. Typical TEM images of the samples which were taken out after adding a fresh mixture of $ZnCl_2$ and Na_2WO_4 to a 40 mL solution containing 0.2 mmol $ZnWO_4$ nanorods and refluxing the mixture for different period. In the synthesis, the nanorods were added into a flask with 50 mL of H_2O, pH 8, and refluxed continuously after adding 1 mL of 0.2 M Na_2WO_4 and 1 mL of 0.2 M $ZnCl_2$. (a) refluxing for 12 h; (b) refluxing for 24 h; (c, e) adding 1 mL 0.2 M Na_2WO_4 and 1 mL 0.2 M $ZnCl_2$ every 12 h. In the third run, the sample was taken out after 3 h. (d) Electron diffraction pattern of the nanorods in (c, e), taking along $\langle 011 \rangle$ zone axis, showing the perfect single-crystal nature.

Such spontaneous "landing" of the small nanoparticles on the backbone of the nanorods and then undergoing self-aggregation instead of the pure aggregation among the small nanoparticles could be related with one proposed mechanism so-called "contact epitaxy" by Averback et al.[16,17] The driving force for this spontaneous oriented attachment is that the elimination of the pairs of high energy surfaces will lead to a substantial reduction in the surface free energy from the thermodynamic viewpoint.[10,13] The initial randomly oriented

SCHEME 2. Proposed Nanorod-Direct Self-Aggregation Process Observed in the Case of $ZnWO_4$ Nanorods under Refluxing Conditions[a]

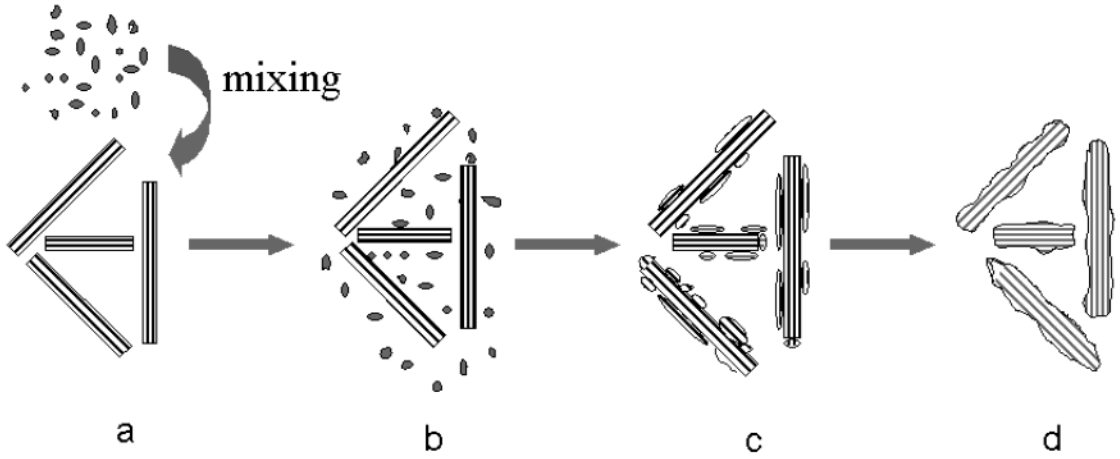

[a] (a and b) The mixing of amorphous nanoparticulates, which are produced from a simple supersaturation precipitation reaction from $ZnCl_2$ and Na_2WO_4 solutions, with well crystallized $ZnWO_4$ nanorods; (c) The directional aggregation of the tiny nanoparticles on the backbone of the nanorods; (d) Well crystallized nanorods with rough surface structures.

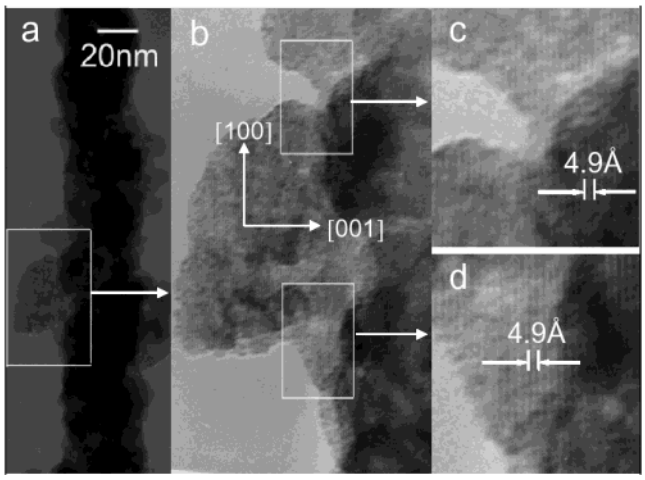

Figure 3. (a) Typical TEM image of the nanorod with rough surface obtained by the refluxing the solution containing the nanorods and the amorphous nanoparticulates. (b) High-resolution TEM of the part as highlighted in (a). (c and d) The lattice resolved HRTEM images of the areas highlighted in (c), showing that all of the small nanoparticles attached on the nanorods taking the same orientation along [100] as the uniaxial of the rods.

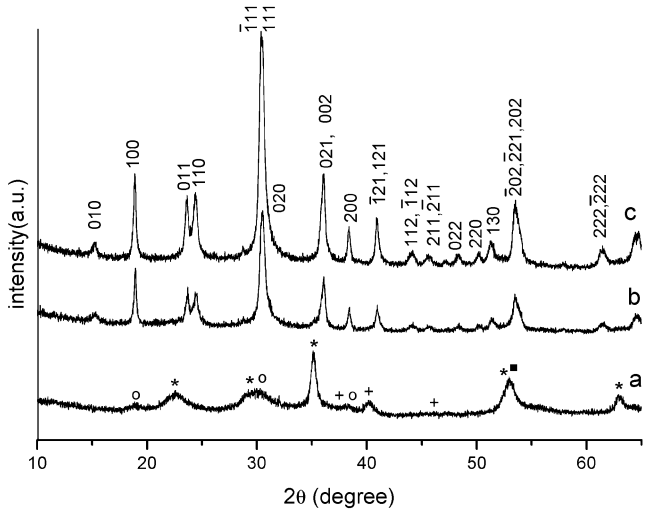

Figure 4. XRD patterns of (a) mixture obtained by refluxing a solution of a fresh mixture with total volume 60 mL after adding 0.2 M $ZnCl_2$ 10 mL of $NaWO_4$ 0.2 M 10 mL, 120 °C, pH 8, for 13 h. * donated Na_2ZnO_3 (JCPDS Card 850325), ■ donated Na_xWO_3 (JCPDS Card 490059), + donated Na_6ZnO_4 (JCPDS Card 702037), ○ donated $ZnWO_4$ (JCPDS Card 150744); (b) $ZnWO_4$ obtained by hydrothermal treatment of a 60 mL aqueous solution after adding 10 mL of 0.2 M $ZnCl_2$ and 10 mL of 0.2 M $NaWO_4$, and 0.2 mmol $ZnWO_4$ nanorods, 120 °C, pH 8, for 12 h; (c) $ZnWO_4$ obtained by hydrothermal treatment of a 60 mL aqueous solution after adding 1 mL of 0.2 M $ZnCl_2$ and 1 mL of 0.2 M $NaWO_4$, 0.2 mmol $ZnWO_4$ nanorods, 180 °C, pH 8, for 12 h.

nanocrystals can align epitaxially with the substrate (refer to nanorods here), which was explained as the rotation of the nanoparticles within the aggregates driven by short-range interactions between adjacent surfaces.[16,17] The so-called nanorod-direct self-aggregation process in our case could be illustrated as in Scheme 2.

In addition, the promoted crystallization and transformation of $ZnWO_4$ precursors in the presence of some amount of single-crystal $ZnWO_4$ nanorods was found. To show the influence of the well crystallized $ZnWO_4$ nanorods on the crystallization and transformation of the amorphous $ZnWO_4$ precursors, the freshly prepared amorphous particles made of fresh $ZnCl_2$ and Na_2WO_4 solutions are refluxed in oil bath or hydrothermally treated at 120 °C, respectively. The XRD pattern in Figure 4a shows that the two samples mainly contain Na_2ZnO_3, Na_xWO_3, $ZnWO_4$, and a small amount of Na_6ZnO_4. The TEM image in Figure 5a shows that the product is composed of tiny nanoparticles with sizes of about 10 nm. In contrast, the control experiment shows that hydrothermal treatment of a fresh mixture at 120 °C for 12 h in the presence of 0.2 mmol single-crystal $ZnWO_4$ nanorods under the same conditions leads to the formation of well crystallized $ZnWO_4$ nanorods with the similar surface structures as obtained under refluxing conditions (see Figures 5b and 2b), implying that the presence of the well crystallized $ZnWO_4$ nanorods can promote the crystallization and transformation of the starting precursor in a form of amorphous nanoparticulates into well crystallized $ZnWO_4$ even at a lower temperature. The results suggested that such induced crystallization and transformation due to the presence of well-crystallized nanorods can effectively decrease the crystallization temperature which is absolutely necessary for the conventional hydrothermal crystallization process in the present case. Figure 5c shows that uniform well crystallized nanorods were produced after hydrothermal treatment of the similar mixture at 180 °C.

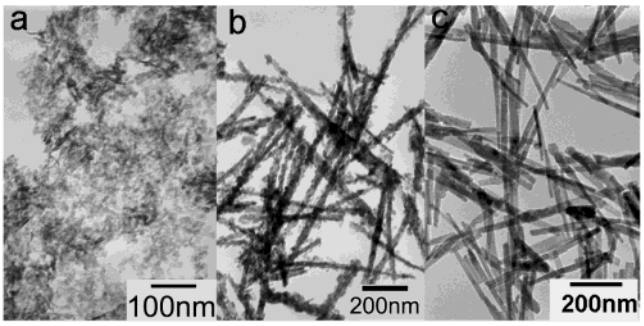

Figure 5. Comparison of the morphology of the nanoparticles produced at the different temperature. TEM images of the nanoparticles obtained by (a) refluxing of a solution made of 10 mL of 0.2 M $ZnCl_2$ and 10 mL of 0.2 M $NaWO_4$, 120 °C, pH 8, for 13 h, without adding singe crystal $ZnWO_4$ nanorods. (b) Hydrothermal treatment of a solution made of 1 mL of 0.2 M $ZnCl_2$ and 1 mL of 0.2 M $NaWO_4$, adding 0.2 mmol $ZnWO_4$ nanorods, 120 °C, pH 8, for 12 h. (c) hydrothermal treatment of a solution made of 1 mL of 0.2 M $ZnCl_2$ and 1 mL of 0.2 M $NaWO_4$, in the presence of 0.2 mmol $ZnWO_4$ nanorods, 180 °C, pH 8, for 12 h.

The TEM image in Figure 5c shows that the nanorods are still straight and their surfaces were smooth with a similar appearance as that found without adding single-crystal $ZnWO_4$ nanorods into the starting mixture made of $ZnCl_2$ and Na_2WO_4 solutions. No obvious nanorod-directed aggregation was found at 180 °C as that observed at 120 °C (Figure 5c). These results suggested that the relative higher temperature was favorable for the formation of the nanorods and that the typical Ostwald ripening process dominates the crystal growth of the nanorods at higher temperature as we discussed before. However, at a relative low temperature, the obvious nanorod-direct oriented attachment mechanism and its promotion of further crystallization and transformation of the nanoparticulates were identified undoubtedly as confirmed by XRD results and electron diffraction patterns.

In summary, we identified that well-crystallized $ZnWO_4$ nanorods can direct the self-aggregation of the amorphous nanoparticulates and promote the crystallization and transformation of the amorphous nanoparticulates derived from a simple supersaturation precipitation reaction in a nanorods/amorphous nanoparticle coexisting system under either refluxing conditions or mild hydrothermal conditions. The obvious nanorod-direct epitaxial aggregation mechanism in this system was clearly observed. Such spontaneous self-aggregation and crystallization induced by the well-crystallized nanorods could provide a unique route for the improving the property of an anisotropic material due to their rough surface structures made of tiny nanoparticle building blocks and could be used for the formation of more complex crystalline three-dimensional structures in which the branching sites could be added as individual nanoparticles.[13,18] We believe that this finding could be universal to various oxide systems or even non-oxide nanorod systems, and further extended study on other oxide nanorod systems is still underway. Further detailed investigation could shed new light on the understanding complicated 1D crystal growth mechanism in solution system.

Acknowledgment. S.-H.Y. thanks, for the special funding support, the Century Program of Chinese Academy of Sciences, the Distinguished Young Fund of the National Science Foundation of China (NSFC, Contract No. 20325104), and NSFC Project No. 50372065 for financial support.

References and Notes

(1) Matijević, E. *Curr. Opin. Colloid Interface Sci*. **1996**, *1*, 176−183.
(2) Sugimoto, T. *Adv. Colloid Interface Sci.* **1987**, *28*, 65−108.
(3) Mullin, J. W. *Crystallization*, 3rd ed.; Butterworth-Heinemann: Oxford, 1997.
(4) Bailey, J. K.; Brinker, C. J.; Mecartney, M. L. *J. Colloid Interface Sci.* **1993**, *157*, 1−13.
(5) Ocana, M.; Morales, M. P.; Serna, C. J. *J. Colloid Interface Sci.* **1995,** *171*, 85−91.
(6) Privman, V.; Goia, D. V.; Park, J.; Matijević, E. *J. Colloid Interface Sci.* **1999**, *213*, 36−45.
(7) Chemseddine, A.; Moritz, T. *Eur. J. Inorg. Chem.* **1999**, 235−245.
(8) Penn, R. L.; Banfield, J. F. *Geochim. Cosmochim. Acta* **1999**, *63*, 1549−1557.
(9) Penn, R. L.; Banfield, J. F. *Science* **1998**, *281*, 969−971.
(10) Banfield, F.; Welch, S. A.; Zhang, H.; Ebert, T. T.; Penn, R. L. *Science* **2000**, *289*, 751−754.
(11) Penn, R. L.; Oskam, G.; Strathmann, T. J.; Searson, P. C.; Stone, A. T.; Veblen, D. R. *J. Phys. Chem. B* **2001,** *105*, 2177−2182.
(12) Penn, R. L.; Stone, A. T.; Veblen, D. R. *J. Phys. Chem. B* **2001**, *105*, 4690−4697.
(13) Alivisatos, A. P. *Science* **2000**, *289*, 736−737.
(14) Onuma, K.; Ito, A. *Chem. Mater.* **1998**, *10*, 3346−3351.
(15) Huang, F.; Zhang, H. Z.; Banfield, J. F. *Nano Lett.* **2003**, *3*, 373−378.
(16) Zhu, H. L.; Averback, R. S. *Philos. Mag. Lett.* **1996**, *73*, 27−33.
(17) Yeadon, M.; Ghaly, M.; Yang, J. C.; Averback, R. S.; Gibson, J. M. *Appl. Phys. Lett.* **1998**, *73*, 3208−3210.
(18) Pacholski, C.; Kornowski, A.; Weller, H. *Angew. Chem., Int. Ed.* **2002**, *41*, 1188−1191.
(19) Chemseddine, A.; Jungblut, H.; Boulmaaz, S. *J. Phys. Chem.* **1996**, *100*, 12546−12551.
(20) Tang, Z. Y.; Kotov, N. A.; Giersig, M. *Science* **2002**, *297*, 237−240.
(21) (a) Chamberland, B. L.; Kafalas, J. A.; Goodenough, J. B. *Inorg. Chem.* **1977**, *16*, 44−46. (b) Gaines, R. V.; Skinner, H. C. W.; Foord, E. E.; Mason, B.; Rosenzweig, A. *Dana's New Mineralogy*, 8th ed.; J. Wiley: New York, 1998; p 993.
(22) (a) Sleight, A. W. *Acta Crystallogr. B* **1972**, *28*, 2899−2902. (b) Fagherazzi, G.; Pernicone, N. *J. Catal*. **1970**, *16*, 321. (c) Moro-Oka, Y.; Ueda, W. In *Advances in Catalysis*; Eley, D. D., Pines, H., Haag, W. O., Eds.; Academic Press: New York, 1994; Vol. 40, p 233.
(23) Yu, S. H.; Liu, B.; Mo, M. S.; Huang, J. H.; Liu, X. M.; Qian, Y. T. *Adv. Funct. Mater.* **2003**, *13*, 639−647.